ELSEVIER

www.elsevier.nl/locate/jorganchem

Journal of Organometallic Chemistry 619 (2001) 164–178

Journal of Organometallic Chemistry

Thioether- and selenoether-carboxylates in palladium chemistry: conclusive proof of hemilabile properties of O–Se ligands

Matthias W. Esterhuysen [a], Robert Brüll [a], Helgard G. Raubenheimer [a,*], Catharine Esterhuysen [a], Gert J. Kruger [b]

[a] *Department of Chemistry, University of Stellenbosch, Private Bag X1, Matieland 7602, South Africa*
[b] *Department of Chemistry and Biochemistry, P.O. Box 524, Auckland Park, Johannesburg 2006, South Africa*

Received 21 December 1999; accepted 18 August 2000

Dedicated to Professor Dr Dr hc Wilhelm Keim on the occasion of his 65th birthday.

Abstract

Reaction of *trans*-[PdCl(Ph)(PPh_3)$_2$] with the thallium salts R–X–$(CH_2)_n$–COOTl ($n = 1$, X = S, R = Me, Et, *i*-Pr, *t*-Bu, Ph; $n = 1$, X = Se, R = Me, Ph; $n = 2$, X = S, R = Et, Ph) yields the compounds *trans*-[Pd(OOC–$(CH_2)_n$–X–R–κ^1-*O*)Ph(PPh_3)$_2$] (**1a**–**1i**). In solution, complexes **1a**–**1i** participate in hemilabile equilibria in which one PPh_3 ligand is replaced by a sulphur/selenium atom of the ligand to afford the O–S/Se chelates under certain circumstances. Solid state structures of the monodentate complex **1h** as well as its corresponding chelate (**2h**) together with the NMR observation of both species in solution, conclusively prove the hemilabile properties of this O–Se ligand. Depending on the size of the substituent on the potential sulphur or selenium donor atom, however, a PPh_3 ligand is not always displaced upon donor atom coordination. In such equilibria no free PPh_3 is detected and a five-coordinate square pyramidal structure is proposed for the O–S/Se chelate. The position of the relevant equilibrium depends on both the basicity of the potential sulphur or selenium donor atom as well as on the polarity of the solvent.

Keywords: Palladium; Arylpalladium complexes; Hemilability; Oxygen–selenium ligands; Oxygen–sulphur ligands

1. Introduction

Recent studies in coordination chemistry have shown considerable interest in the use of so-called hemilabile ligands [1]. Hemilabile ligands generally have at least two different potential donor atoms, e.g. phosphorus and oxygen, enabling the formation of complexes in which one donor atom is strongly bonded whilst the other is more loosely coordinated [2]. According to the generally accepted theory, the latter donor atom can dissociate from the metal so that the ligand binds in a monodentate mode, vacating a coordination site for a potential substrate [3,4]. Palladium complexes with hemilabile ligands are known to exhibit interesting catalytic properties, especially in C–C bond formation processes where it is currently believed that the dissociation of the chelate ring to create one free coordination position is initiated 'on demand' by either substrate monomers or coordinating solvent molecules [3] (Scheme 1).

While the hemilabile behaviour of P–O ligands has been well investigated and substantiated by spectroscopic methods [1,3,5], much less is known about potentially hemilabile P–N [6–9], P–S [10,11], O–N [12–14], O–O [13] and O–S [13] ligands. The hemilabile properties of a few thioethercarboxylate ligands in palladium chemistry have recently been investigated

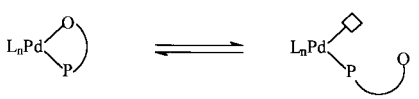

□ = free coordination position

Scheme 1. Availability of a free coordination position with hemilabile P–O ligands.

* Corresponding author. Tel.: +27-21-8083850; fax: +27-21-8083849.
E-mail address: hgr@land.sun.ac.za (H.G. Raubenheimer).

0022-328X/01/$ - see front matter
PII: S0022-328X(00)00571-4

in our group [15]. The work focused on hemilabile equilibria in which neutral sulphur atoms in monodentately, oxygen-bonded ligands coordinate to palladium while replacing a triphenylphosphine ligand. These substitutions were studied in solution by means of $^{31}P\{^{1}H\}$-NMR spectroscopy and the subsequent hemilabile equilibria could be observed by peak broadening. Crystallization, however, failed to produce the proposed bidentate O–S chelates and only the oxygen-bonded complexes were isolated.

The aim of the current work was not only to extend the knowledge concerning the occurrence of hemilabile equilibria, but also to isolate and structurally characterize the postulated coordination types in such equilibria. In this paper we thus describe a continuation and extension of the above-mentioned study involving the synthesis and characterization of phenylpalladium compounds bearing alkyl and aryl thioethercarboxylate O–S-type, as well as alkyl- and aryl-selenoethercarboxylate O–Se-type, ligands. Molecular structures of O–S/Se ligated complexes, showing the potentially bidentate ligands in both monodentate and bidentate bonding modes, are presented. Solid state structures of the monodentate complex **1h** as well as its resulting chelate (**2h**), together with the observation that they are in equilibrium when dissolved conclusively prove the hemilabile properties of this O–Se ligand in solution. Furthermore, different hemilabile behaviour for sulphur- and selenium-donor atom coordination to palladium observed spectroscopically in solution, is presented. The effect of chelate ring size has also been investigated.

2. Results and discussion

2.1. Synthesis of bis(triphenylphosphine)phenylpalladium(II) complexes with hemilabile O–S and O–Se ligands

The new phenylpalladium complexes **1a**–**1i** were prepared by the general procedure outlined in Scheme 2. Precipitation of TlCl with excess thallium salt of a ligand drove the reaction. The complexes **1a**, **1b**, **1e**, **1h**, **1i** were isolated in good and **1c**, **1d**, **1f**, **1g** in moderate yields by crystallization from THF/pentane. Characterization data for all the new compounds appear in Section 3. As a result of the dynamic equilibria observed it was not always possible to assign all the signals in the $^{13}C\{^{1}H\}$-NMR spectra.

The crystal and molecular structures of **1a** and its selenium analogue **1h** were determined by single crystal X-ray diffraction and they clearly exhibited uncoordinated sulphur and selenium atoms (Figs. 3 and 5). Prolonged crystallization from THF/pentane or benzene/pentane at low temperatures yielded small amounts ($<5\%$) of dark-yellow crystals amongst colourless crystals of **1a** and **1h**. Elemental analyses as well as single crystal X-ray diffraction studies identified these compounds as the O–S/Se chelate complexes **2a** and **2h** (Figs. 4 and 6). In both compounds a coordinated sulphur/selenium group substituted a phosphine ligand.

2.2. $P\{^{1}H\}$-NMR spectroscopic characterization of complexes 1a–1i

The diphosphine complexes **1a**–**1i** all exhibit NMR signals for coordinated PPh_3 ligands in their room temperature $^{31}P\{^{1}H\}$-NMR spectra ($CDCl_3$). These peaks appear at δ 21.5 for **1c**, **1d** and **1h** and their broadness suggests the presence of dynamic phenomena (Section 3). In addition, the same complexes each exhibit equally broad peaks for free PPh_3 at approximately δ −4.7, and another similarly broad peak with roughly the same intensity at δ 25.2, 26.0 and 27.3 (Fig. 1) corresponding to coordinated PPh_3 in the formed chelates. For **1h** the latter two peaks appear only at low temperature (−40°C) as the exchange rate is too fast for the NMR instrument to distinguish between the species involved in the equilibrium (Scheme 3) at higher temperatures.

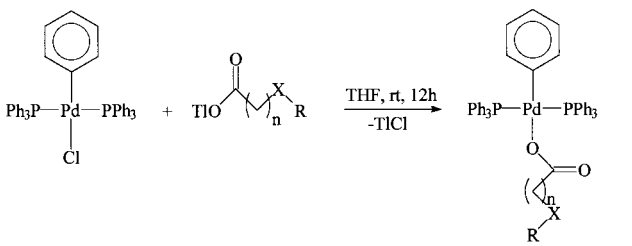

	R	n	X
1a	Me	1	S
1b	Et	1	S
1c	*i*-Pr	1	S
1d	*t*-Bu	1	S
1e	Ph	1	S
1f	Et	2	S
1g	Ph	2	S
1h	Me	1	Se
1i	Ph	1	Se

Scheme 2. Preparation of phenylpalladium(II) compounds **1a**–**1i**.

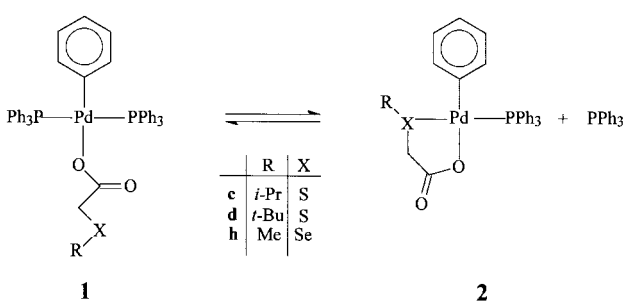

Scheme 3. Hemilabile equilibrium with PPh_3 exchange.

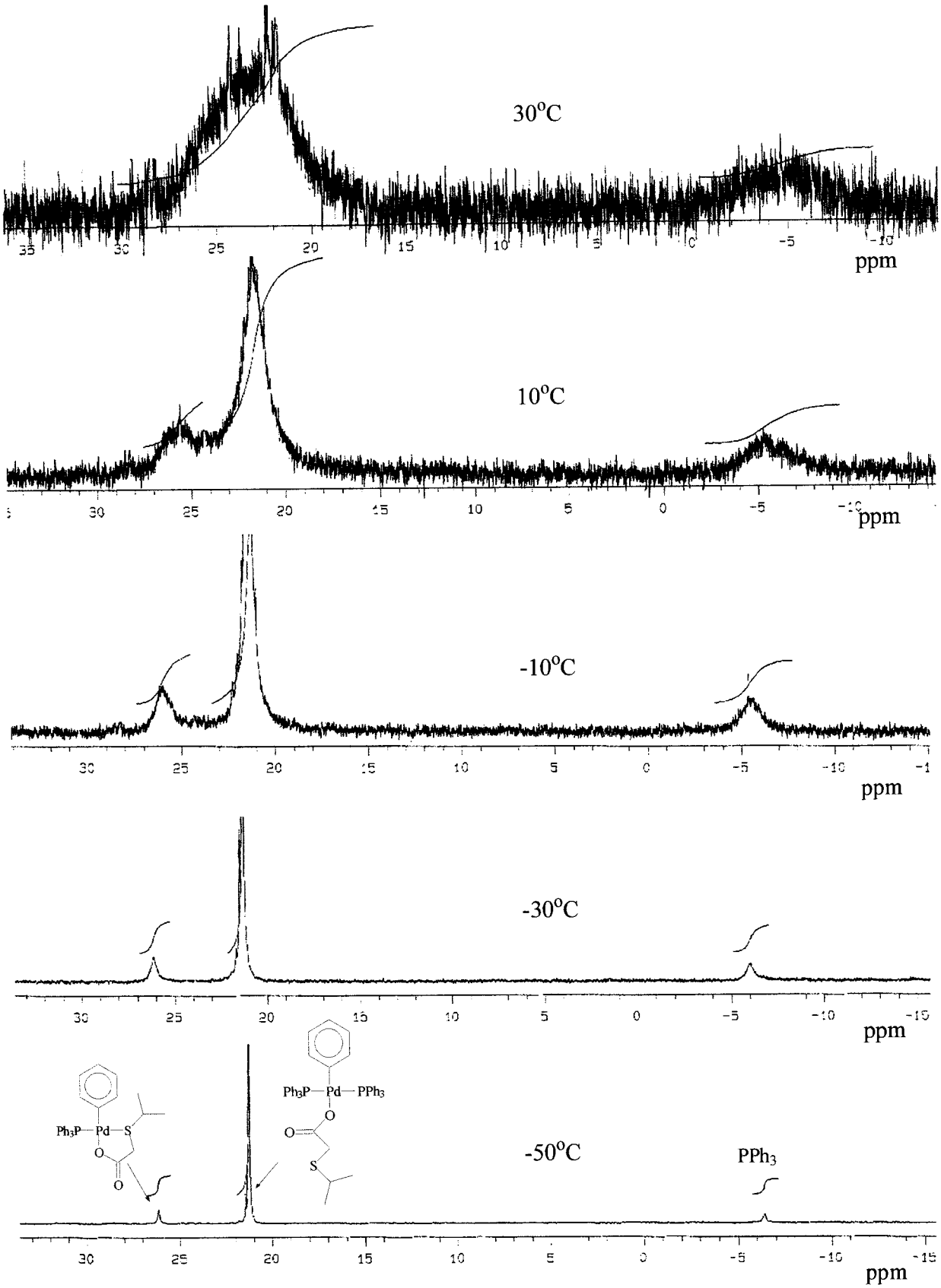

Fig. 1. Variable temperature $^{31}P\{^{1}H\}$-NMR spectra of **1c** exhibiting hemilabile equilibrium.

The room temperature $^{31}P\{^{1}H\}$-NMR spectra ($CDCl_3$) of **1a**, **1b**, **1e**, **1f**, **1g** and **1i** also exhibit extremely broad peaks (up to 14 ppm wide for **1b**). However, no free PPh_3 is indicated in any of these spectra. Resonances, probably due to PPh_3 in O–S chelated species at δ 23.9 appear downfield from the signals for PPh_3 in the non-chelated species in the spectra of **1f** and **1g**. For complexes **1a**, **1b**, **1e** and **1i** only one very broad signal is observed at δ 22.5, 22.0, 21.5 and 23.0, representing PPh_3 in the chelated and non-chelated species involved in the equilibria. With C_6D_6 as solvent these peaks sharpen, indicating slower exchange rates. For example **1e**, **1f** and **1g** exhibit well defined room temperature signals for PPh_3 in the O–S chelated species at δ 25.7, 23.3 and 23.2. For **1a**, **1b** and **1i**, however, only a single broad signal is still present. Cooling the NMR samples ($CDCl_3$) of **1a** and **1b** down to -60°C enabled the observation of $^{31}P\{^{1}H\}$-NMR

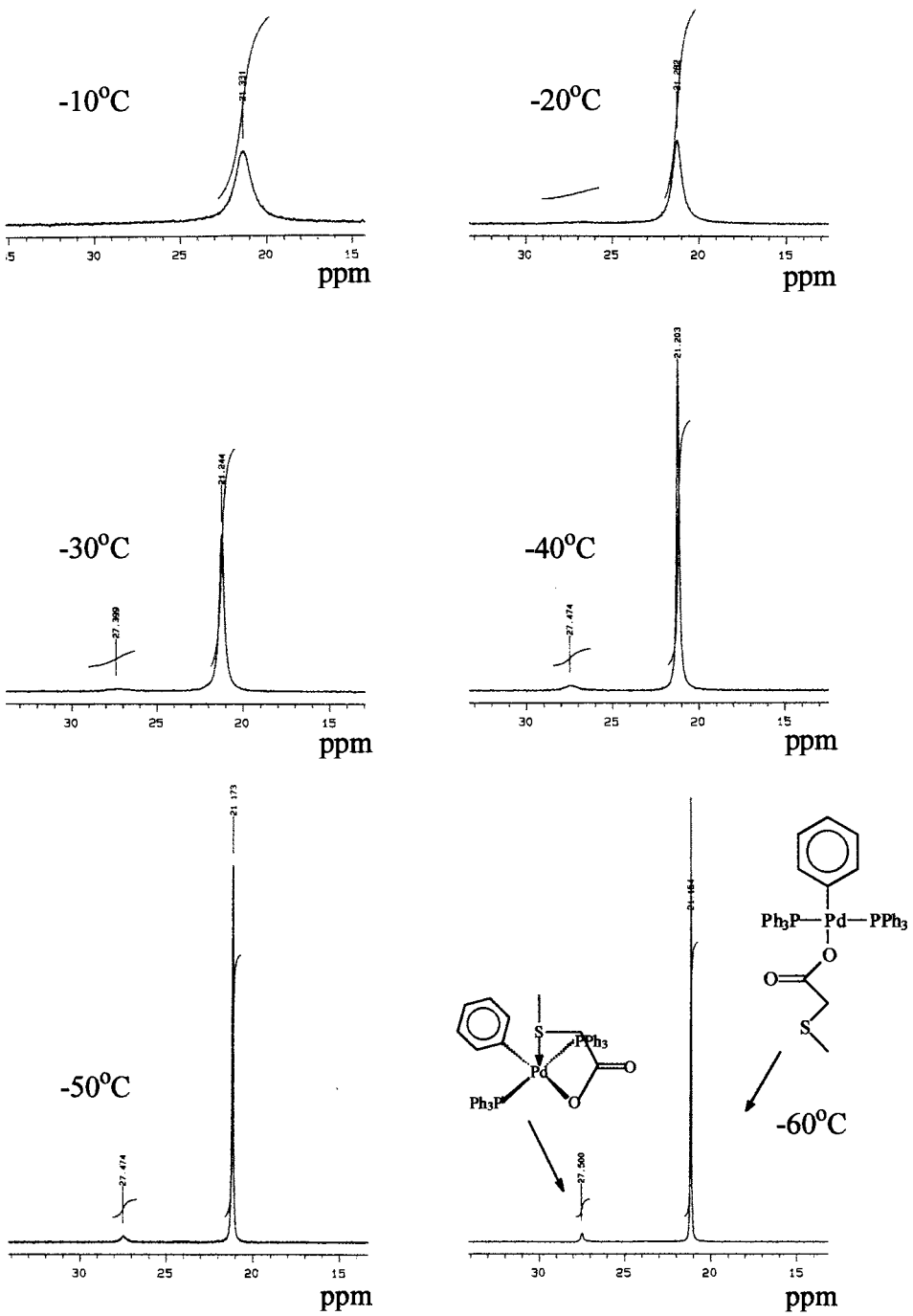

Fig. 2. Variable temperature $^{31}P\{^{1}H\}$-NMR spectra of **1a**.

signals at δ 27.5 (Fig. 2) and 26.6 for PPh_3 probably in a chelated species participating in a non-substitutive equilibrium.

The absence of free PPh_3, together with the presence of signals for PPh_3 in a new species in the equilibria of **1a**, **1b**, **1e**, **1f** and **1g**, appearing downfield from the signals for PPh_3 in the non-chelated species, indicates that these complexes probably participate in a associative hemilabile equilibrium but that the S or Se coordination is not accompanied by PPh_3 substitution (Scheme 4). An $18e^-$ five-coordinate square pyramidal structure of type **3** is plausible. Ab initio and empirical calculations are currently being undertaken in an effort to strengthen our postulate. Although $18e^-$ five-coordinate square pyramidal structures have been proposed as transtion states during substitution reactions for many organometallic palladium complexes [16–18], only one example is known where this species could be isolated and structrally characterized by X-ray diffraction [19].

The formation of **2a** and **2h** upon crystallization instead of the spectroscopically observed species, **3a** and **3h**, indicates that PPh_3 substitution occurs during crystal formation.

2.3. Infrared spectroscopic characterization of complexes *1a–1i*

The asymmetric ν(CO) stretching vibrations for the carboxyl group of the O–S/Se ligands in complexes **1a–1i** are found between 1600 and 1628 cm^{-1}, typically at lower energy than for the corresponding free carboxylic acids. This can be ascribed to coordination and partial electron loss from the carboxylate ligand to palladium. A 21 cm^{-1} 'red shift' is observed between the $\nu(CO)_{as}$ absorption bands going from **1a** (1610 cm^{-1}) to **2a** (1631 cm^{-1}) and from **1h** (1600 cm^{-1}) to **2h** (1621 cm^{-1}), indicating lower π-bond character of the C=O-bond in the chelated compounds. The values for $\nu(CO)_{as}$ also correspond to the positions of the same vibrations in the palladium thioethercarboxylates previously studied (1595–1608 cm^{-1}) [15].

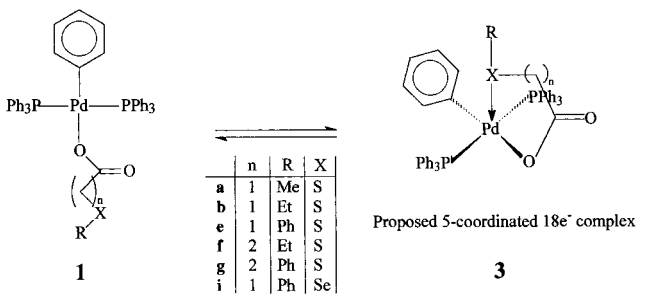

Scheme 4. Proposed equilibrium with no PPh_3 exchange.

2.4. Crystal and molecular structures of *1a*, *1h*, *2a* and *2h*

The molecular structures of complexes **1a**, **1h**, **2a** and **2h** are shown in Figs. 3–6. For clarity the disorder exhibited by the carboxylate ligands in the crystal structures of **1a** and **1h** and the solvent inclusions found in the structures of **1h**, **2a** and **2h** are not shown in the figures.

The molecular structures of the monodentate forms **1a** and **1h** on the one hand and the bidentate forms **2a** and **2h** on the other hand closely resemble each other. The bond lengths and angles observed for **1a** and **1h** are the same within three standard deviations of the average, except for the expected differences between the two S–C bond lengths in **1a** and the Se–C bond lengths in **1h**. The same is true for **2a** and **2h** with the bond lengths and angles in the phenyl ligand and remaining triphenylphosphine ligand (one triphenylphosphine ligand was lost upon coordination of the S/Se atoms) also being very similar to their monodentate counterparts. All four structures exhibit a square-planar configuration around the Pd atom, which is slightly deformed in **2a** and **2h** as a result of the ring strain in the five-membered chelate rings (maximum deviations from planarity of 0.081(1) and 0.110(1) Å respectively). Smaller O(1)–Pd–S/Se angles are found in the type **2** structures (83.9/84.9°) compared to the O(1)–Pd–P angles in structures of type **1** (91.9/91.9° and 95.4/92.4° for O(1)–Pd–P(1) and O(1)–Pd–P(2) in **1a** and **1h** respectively). The positions of the oxygen atoms are more affected by the ring strain and the C(4)–Pd–O(1) angles in **2a** and **2h** deviate significantly from linearity (170.9 and 170.0°), whereas the P–Pd–S/Se angles are closer to linearity (175.3 and 174.2°). All the internal ligand angles between atoms in the chelate ring are also slightly larger than their non-chelated counterparts as a result of the strain.

The phenyl ligand coordinated to the palladium is twisted with respect to the plane through the Pd, P(1), P(2), C(4) and O(1) atoms. In the non-chelated structures (**1a** and **1h**) it is almost perpendicular to the plane (88.6 and 88.9° away), while in the chelated structures (**2a** and **2h**) it is rotated by only 73.9° (**2a**) and 75.4° (**2h**), presumably as a result of the extra space created by the absence of the second triphenylphosphine ligand. For structures **1a** and **1h** this effect can also be observed in the carboxylate ligand, where O(1), C(1), O(2) and C(2) form a plane which is nearly co-planar to the phenyl ring (11.9 and 3.7° difference in **1a** and **1h** respectively). There is, furthermore, an internal pseudo-mirror plane through the phenyl ring and atoms O(1), O(2) and C(1) of the carboxylate ligand in **1h**, with the disordered atoms related to each other across it.

In structures **2a** and **2h** the planar carboxylate ligands are twisted at angles of 14 and 16° respectively to

the planes through P, S or Se, C(4) and O(1). The methyl groups attached to the S or Se atoms (C(3)), however, lie well above this plane.

In structures **2a** and **2h** the molecules pack in strings with the chelate rings parallel but alternating in orientation and with solvent molecules (THF in **2a** and benzene in **2h**) sandwiched in between the rings.

3. Experimental

3.1. General, materials and measurement

Reactions and manipulations involving organometallic compounds were carried out under a dry nitrogen atmosphere using standard Schlenk and vacuum-line techniques. All solvents, except methanol, were dried and purified by conventional methods and freshly distilled under nitrogen shortly before use. Other reagents were used without further purification.

The palladium starting complex, *trans*-[PdCl(Ph)(PPh_3)$_2$] [20], and the ligands, $R^1S–CH_2–COOH$ (R^1 = Et [21], *i*-Pr [22], *t*-Bu [23], Ph [24]), $R^2S–(CH_2)_2–COOH$ (R^2 = Et [25], Ph [26]) and $R^3Se–CH_2–COOH$ (R^3 = Me [27], Ph [28]) were prepared according to literature methods. (Methylthio)acetic acid was purchased from Aldrich and used without further purification. Melting points were determined on a Büchi 535 apparatus. NMR spectra (^{1}H at 300 MHz, $^{13}C\{^1H\}$ at 75 MHz with Me_4Si as internal standard and $^{31}P\{^1H\}$-NMR at 121 MHz with 85% H_3PO_4 as external standard) were recorded on a Varian VXR 300 FT NMR spectrometer. ^{77}Se $\{^1H\}$-NMR spectra (at 76 MHz with 20% $Se(CH_3)_2$ in d_1-chloroform as external standard) were measured on a Bruker Avance DXR 400 FT NMR spectrometer. NMR peaks are labelled as singlet (s), doublet (d), triplet (t), multiplet (m) or broad (br). In NMR spectra where more than one species is detected, peaks are assigned to the proposed S or Se coordinated and not coordinated compounds. FAB-MS was recorded on a Micromass DG 70/70E mass spectrometer using xenon gas as bombardment atoms. IR data (4000 to 600 cm^{-1}, resolution 4 cm^{-1}) were measured as KBr pellets of recrystallized samples using a Perkin–Elmer 841 IR spectrophotometer. Peaks are described as very strong (vs), strong (s), medium (m) or weak (w) in intensity. Elemental analyses were carried out by the Division of Energy Technology, CSIR, Pretoria, South Africa.

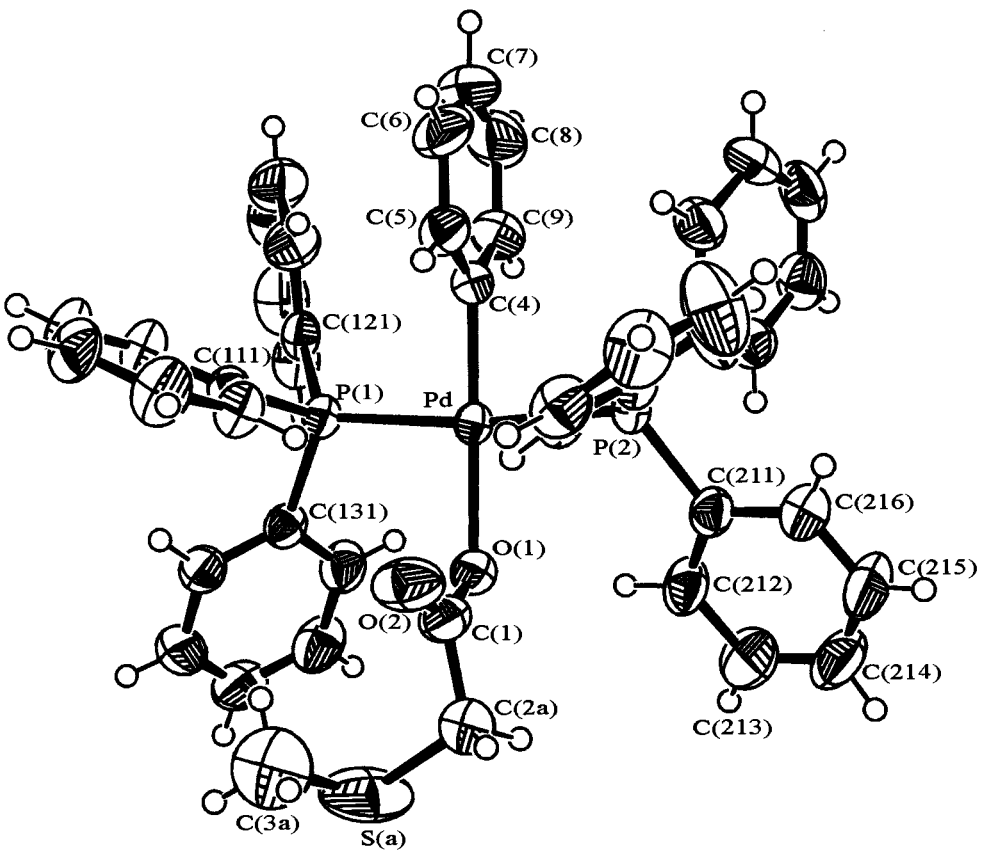

Fig. 3. ORTEP plot of the molecular structure of complex **1a** (one of two disordered configurations), showing the numbering scheme.

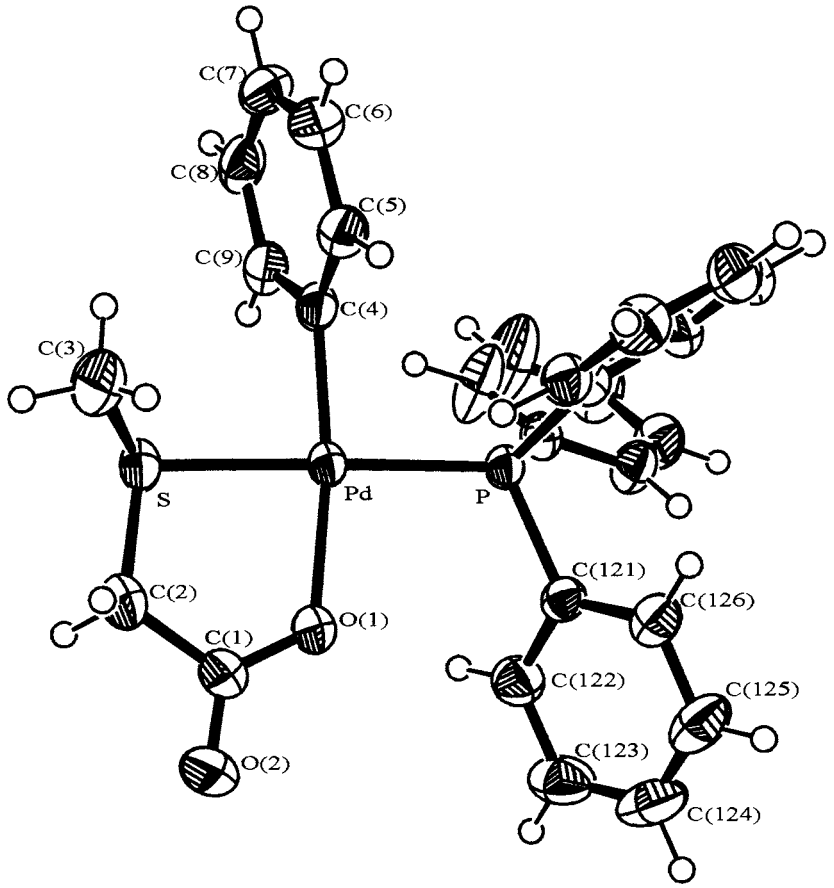

Fig. 4. ORTEP plot of the molecular structure of complex **2a**, showing the numbering scheme.

*3.2. Crystal structure determinations of **1a**, **1h**, **2a** and **2h***

Crystals of **1a** and **1h**, suitable for X-ray crystallographic analysis, were obtained by crystallization from THF/pentane. Prolonged crystallization of **1a** and **1h** from THF/pentane, furthermore, yielded small amounts of **2a** and **2h** among **1a** and **1h**. Diffraction data of **1a**, **1h** and **2a** were collected on a Siemens SMART system with CCD detector at room temperature, using graphite monochromated Mo–K_α radiation. Empirical absorption corrections were applied using the Siemens utility program SADABS for CCD detectors [29]. Diffraction data of **2h** were collected on a Philips PW1100 diffractometer, controlled by the program PWPC [30], at room temperature using ω–2θ scans and graphite monochromated Mo–K_α radiation. Data reduction and absorption corrections were performed with the XTAL3.4 suite of programs (DIFDAT and ABSCAL) [31].

All structures were solved by interpretation of a Patterson synthesis, which yielded the positions of the metal atoms. The remaining non-hydrogen atoms were found by difference Fourier map. Those atoms in non-disordered sites were refined by full-matrix least-squares and allowed anisotropic thermal displacement motion. The disordered atoms in the carboxyl ligands of **1a** and **1h** were also located by difference Fourier mapping, and refined individually, with all atoms except for the disordered C1 and C2 sites in **1h** given anisotropic thermal displacement parameters. The disordered solvent molecules in **1a**, **1h** and **2a** were initially refined as rigid bodies. The rigid body constraints were then lifted and the bond lengths restrained to average literature distances listed in the International Tables for Crystallography [32], during isotropic refinement. It was possible to locate most of the non-solvent hydrogen atoms by Fourier map.

SHELX-97 [33] was used to solve and refine the structures and to generate the tables. ORTEP-3 [34] was used to generate the figures at 50% probability level. Final values for the residuals of R, wR and S in **1a**, **1h**, **2a** and **2h** are listed in Table 1 together with crystal data, refinement data and data collection parameters. Important bond lengths and angles in **1a**, **1h**, **2a** and **2h** are listed in Tables 2 and 3. Fractional coordinates and equivalent isotropic displacement parameters of all atoms in the respective structures are listed in Tables 4–7.

3.3. Preparation of *trans*-[Pd(OOC–CH_2–SR–κ^1-O)Ph(PPh_3)$_2$] (**1a** R = Me; **1b** R = Et; **1c** R = i-Pr; **1d** R = t-Bu; **1e** R = Ph)

To a solution of RS–CH_2–COOH (0.48 mmol, R = Me, Et, *i*-Pr, *t*-Bu, Ph) in 15 ml methanol was added 113 mg (0.24 mmol) Tl_2CO_3. The solution was stirred at room temperature until all the Tl_2CO_3 dissolved, after which the solvent was removed in vacuo. The remaining thallium salt was dried for a further 30 min in vacuo and subsequently manipulated under nitrogen. The thallium salt was suspended in 15 ml THF and after adding *trans*-[PdCl(Ph)(PPh_3)$_2$] (200 mg, 0.27 mmol) the mixture was stirred for 12 h at room temperature. Precipitated TlCl and unreacted thallium salts were filtered off through a Celite pad. The volume of the colourless to light red solutions was reduced in vacuo to approximately 3 ml. Careful layering of the concentrated solutions with pentane, followed by cooling to −5°C, afforded colourless to light orange crystals of complexes **1a**–**1e**. Yields were in the range of 45 to 80% without attempting further crystallization from the mother liquid.

trans-[Pd(OOC–CH_2–SMe–κ^1-*O*)Ph(PPh_3)$_2$] (**1a**). Colourless crystals in 80% yield, m.p. 174°C (dec.). ^{1}H-NMR δ (d_1-chloroform, 298 K): 1.6 (br, 3H, SCH_3), 2.6 (br, 2H, CH_2S), 6.88 (d, 2H, ^3J 8.1 Hz, Pd–C_6H_5), 6.35 (t, 2H, ^3J 7.5 Hz, Pd–C_6H_5), 6.52 (t, 1H, ^3J 7.5 Hz, Pd–C_6H_5), 7.0–7.5 (m, 30H, Pd–P(C_6H_5)$_3$). ^{13}C{^{1}H}-NMR δ (d_1-chloroform, 298 K): 16.2 (SCH_3), 39.5 (CH_2S), 122.3 (Pd–C_6H_5), 127.6 (Pd–C_6H_5), 128.3 (Pd–P(C_6H_5)$_3$), 130.0 (Pd–P(C_6H_5)$_3$), 131.3 (Pd–C_6H_5), 135.0 (Pd–P(C_6H_5)$_3$), 137.9 (Pd–P(C_6H_5)$_3$), 148.6 (Pd–C_6H_5), 173.6 (Pd–OCO). ^{31}P{^{1}H} δ (d_1-chloroform, 298 K): 20–25 (br). IR (KBr): ν_{as}(CO) 1610 cm^{-1} (vs). FAB-MS: *m*/*z* 813 [M$^+$]. Anal. Calc. for $C_{45}H_{40}P_2PdO_2S$: C, 66.5; H, 5.0; S, 3.9. Found: C, 66.6; H, 5.1; S, 3.8%.

trans-[Pd(OOC–CH_2–SEt–κ^1-*O*)Ph(PPh_3)$_2$] (**1b**). Light yellow crystals in 75% yield, m.p. 168°C (dec.). ^{1}H-NMR δ (d_1-chloroform, 298 K): 1.0 (br, 3H, SCH_2CH_3), 2.1 (br, 2H, SCH_2CH_3), 2.6 (br, 2H, $OOCCH_2S$), 6.63 (d, 2H, ^3J 7.2 Hz, Pd–C_6H_5), 6.38 (t, 2H, ^3J 6.9 Hz, Pd–C_6H_5), 6.54 (t, 1H, ^3J 7.2 Hz, Pd–C_6H_5), 7.2–7.4 (m, 30H, Pd–P(C_6H_5)$_3$). ^{13}C{^{1}H}-NMR δ (d_1-chloroform, 298 K): 14.1 (CH_3), 27.4 (SCH_2), 36.8 (CH_2), 122.2 (Pd–C_6H_5), 127.2 (Pd–C_6H_5), 128.1 (Pd–P(C_6H_5)$_3$), 129.7 (Pd–P(C_6H_5)$_3$), 131.2 (Pd–C_6H_5), 134.3 (Pd–P(C_6H_5)$_3$), 136.7 (Pd–P(C_6H_5)$_3$), 146.4 (Pd–C_6H_5), 174.7 (Pd–OCO). ^{31}P{^{1}H} δ (d_1-chloroform, 298 K): 15–29 (br). IR (KBr): ν_{as}(CO) 1609 cm^{-1} (vs). Anal. Calc. for $C_{46}H_{42}P_2PdO_2S$: C, 66.8; H, 4.6; S, 3.9. Found: C, 66.6; H, 4.7; S, 3.9%.

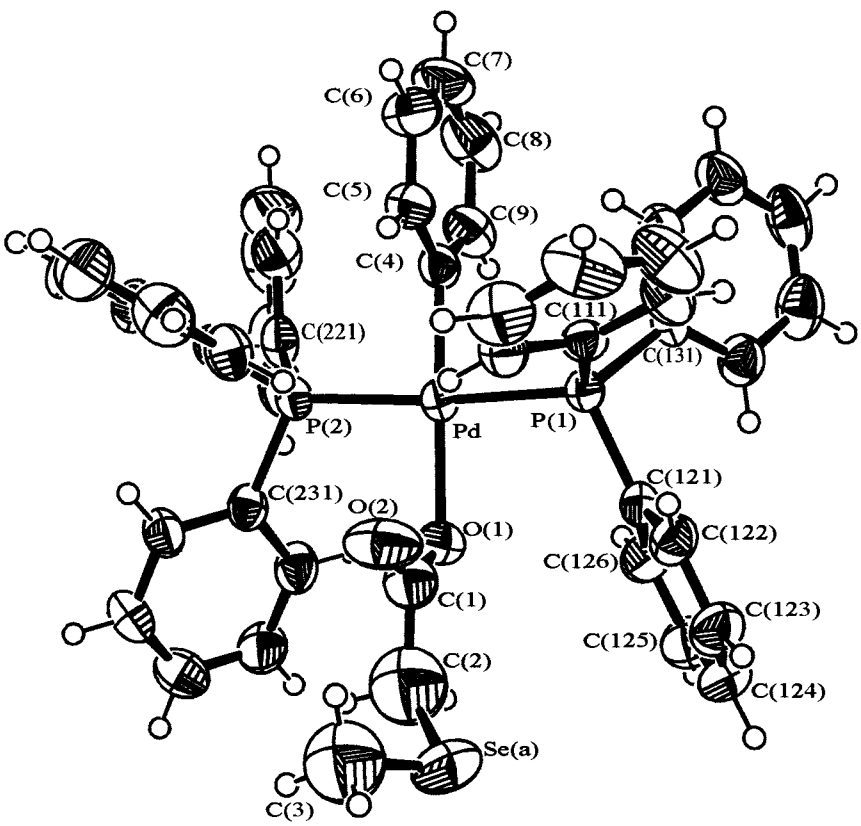

Fig. 5. ORTEP plot of the molecular structure of complex **1h** (one of two disordered configurations), showing the numbering scheme.

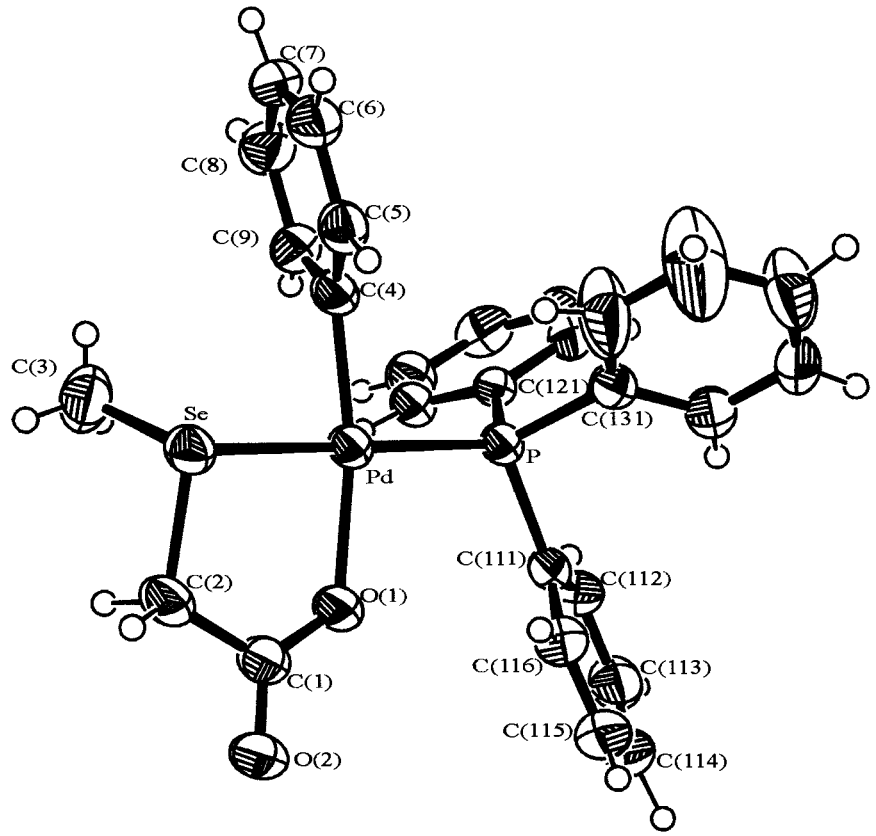

Fig. 6. ORTEP plot of the molecular structure of complex **2h**, showing the numbering scheme.

trans-[Pd(OOC–CH_2–S*i*-Pr–κ^1-*O*)Ph(PPh_3)$_2$] (**1c**). Colourless crystals in 45% yield, m.p. 132°C (dec.). ^{1}H-NMR δ (d_1-chloroform, 298 K): 1.1 (br, 6H, $C(CH_3)_2$), 2.7 (br, 3H, SCH and CH_2S), 6.71 (d, 2H, ^3J 7.2 Hz, Pd–C_6H_5), 6.44 (t, 2H, ^3J 6.9 Hz, Pd–C_6H_5), 6.56 (t, 1H, ^3J 7.1 Hz, Pd–C_6H_5), 7.2–7.5 (m, 30H, Pd–P(C_6H_5)$_3$). ^{13}C{^{1}H}-NMR δ (d_1-chloroform, 298 K): 14.1 (CH_3), 22.8 (SCH), 35.4 (CH_2), 122.4 (Pd–C_6H_5), 127.3 (Pd–C_6H_5), 128.2 (Pd–P(C_6H_5)$_3$), 129.7 (Pd–P(C_6H_5)$_3$), 134.3 (Pd–P(C_6H_5)$_3$), 136.5 (Pd–P(C_6H_5)$_3$), 146.2 (Pd–C_6H_5), 177.3 (Pd–OCO). ^{31}P{^{1}H} δ (d_1-chloroform, 298 K): 19.5–23.5 (br, S not coordinated), 23.5–27.0 (br, S coordinated). IR (KBr): ν_{as}(CO) 1601 cm^{-1} (vs). Anal. Calc. for $C_{47}H_{44}P_2PdO_2S$: C, 67.1; H, 5.3; S, 3.8. Found: C, 67.3; H, 5.3; S, 3.7%.

trans-[Pd(OOC–CH_2–S*t*-Bu–κ^1-*O*)Ph(PPh_3)$_2$] (**1d**). Colourless crystals in 45% yield, m.p. 150°C (dec.). ^{1}H-NMR δ (d_1-chloroform, 298 K): 1.3 (br, 9H, $SC(CH_3)_3$), 3.6 (br, 2H, CH_2S), 6.9 (br, 2H, Pd–C_6H_5), 6.3 (br, 2H, Pd–C_6H_5), 7.2–7.6 (m, 31H, Pd–P(C_6H_5)$_3$ and Pd–C_6H_5). ^{13}C{^{1}H}-NMR δ (d_1-chloroform, 298 K): 30.3 (SCH_2), 35.9 (CH_3), 52.0 (SC), 122.7 (Pd–C_6H_5), 127.3 (Pd–C_6H_5), 128.3 (Pd–P(C_6H_5)$_3$), 130.4 (Pd–P(C_6H_5)$_3$), 134.4 (Pd–P(C_6H_5)$_3$), 137.0 (Pd–P(C_6H_5)$_3$), 145.2 (Pd–C_6H_5), 177.5 (Pd–OCO). ^{31}P{^{1}H} δ (d_1-chloroform, 298 K): 20.5–22.5 (br, S not coordinated), 25–27 (br, S coordinated). IR (KBr): ν_{as}(CO) 1628 cm^{-1} (vs). Anal. Calc. for $C_{48}H_{46}P_2PdO_2S$: C, 67.4; H, 5.4; S, 3.8. Found: C, 67.7; H, 5.6; S, 3.7%.

trans-[Pd(OOC–CH_2–SPh–κ^1-*O*)Ph(PPh_3)$_2$] (**1e**). Colourless crystals in 70% yield, m.p. 127°C (dec.). ^{1}H-NMR δ (d_1-chloroform, 298 K): 2.7 (br, 2H, CH_2S), 6.97 (d, 2H, ^3J 8.1 Hz, Pd–C_6H_5), 6.52 (t, 2H, ^3J 9.0 Hz, Pd–C_6H_5), 6.31 (t, 1H, ^3J 7.5 Hz, Pd–C_6H_5), 6.8–7.8 (m, 35H, Pd–P(C_6H_5)$_3$ and SC_6H_5). ^{13}C{^{1}H}-NMR δ (d_1-chloroform, 298 K): 38.6 (SCH_2), 122.0 (Ph), 124.3 (Ph), 127.1 (Ph), 127.3 (Ph), 128.1 (Ph), 129.8 (Ph), 131.9 (Ph), 132.1 (Ph), 134.5 (Ph), 137.3 (Ph), 146.0 (Ph), 146.4 (Ph), 172.2 (Pd–OCO). ^{31}P{^{1}H} δ (d_1-chloroform, 298 K): 21.5 (br). IR (KBr): ν_{as}(CO) 1615 cm^{-1} (vs). FAB-MS: m/z 721 [$M^+ - 2Ph$]. Anal. Calc. for $C_{50}H_{42}P_2PdO_2S$: C, 68.6; H, 4.8; S, 3.7. Found: C, 68.7; H, 4.9; S, 3.6%.

3.4. Preparation of *trans*-[Pd(OOC–CH_2–SMe–κ^2-*O*,*S*)Ph(PPh_3)] (**2a**)

Prolonged crystallization of **1a** from THF–pentane at −5°C afforded small amounts of dark yellow crys-

Table 1
Crystal data and structure refinement

Identification code	**1a**	**2a**
Empirical formula	$C_{45}H_{40}O_2P_2PdS$	$C_{27}H_{25}O_2PPdS\cdot\frac{1}{2}THF$
Formula weight	813.25	586.95
Temperature (K)	293(2)	293(2)
Radiation, wavelength (Å)	Mo–K_α, 0.71073	Mo–K_α, 0.71073
Crystal system, space group	Monoclinic, $P2_1/n$	Triclinic, $P\bar{1}$
Unit cell dimensions		
a (Å)	15.9232(7)	9.872(2)
b (Å)	15.8426(7)	10.266(4)
c (Å)	16.2958(8)	14.579(3)
α (°)	90	85.00(2)
β (°)	109.124(1)	71.561(18)
γ (°)	90	68.76(2)
Volume (Å^3)	3884.0(3)	1305.7(6)
Z, calculated density (Mg m^{-3})	4, 1.391	2, 1.493
Reflections for cell parameters	19771	7900
Absorption coefficient (mm^{-1})	0.642	0.828
Absorption correction method	Empirical (SADABS)	Empirical (SADABS)
T_{min}	0.75	0.72
T_{max}	0.83	0.86
$F(000)$	1672	600
Crystal size (mm)	$0.48\times0.38\times0.30$	$0.50\times0.33\times0.18$
Crystal colour	Colourless	Yellow
Diffractometer type	Siemens SMART system	Siemens SMART system
Scan type	Area detector	Area detector
θ range for data collection (°)	1.35–25.00	2.13–27.00
Index ranges		
	$-18\le h\le 9$ $-18\le k\le 18$ $-17\le l\le 19$	$-12\le h\le 6$ $-13\le k\le 12$ $-18\le l\le 17$
Reflections collected/unique	19771/6770 [$R_{int}=0.0291$]	7900/5451 [$R_{int}=0.0151$]
Refinement method	Full-matrix least-squares on F^2	Full-matrix least-squares on F^2
Data/restraints/parameters	6770/0/601	5451/5/409
Goodness-of-fit on F^2 (S)	1.037	1.047
Final R indices [$I>2\sigma(I)$]	$R_1=0.0317$, $wR_2=0.0656$	$R_1=0.0291$, $wR_2=0.0711$
R indices (all data)	$R_1=0.0471$, $wR_2=0.0601$	$R_1=0.0346$, $wR_2=0.0748$
Weighting scheme	calc $w=1/[\sigma^2(F_o^2)+(0.0181P)^2+2.5082P]$ where $P=(F_o^2+2F_c^2)/3$	calc $w=1/[\sigma^2(F_o^2)+(0.0336P)^2+0.9083P]$ where $P=(F_o^2+2F_c^2)/3$
Maximum shift/esd	0.001	0.092
Largest difference peak and hole (e Å^{-3})	0.273 and −0.285	0.379 and −0.470
Identification code	**1h**	**2h**
Empirical formula	$C_{45}H_{40}O_2P_2PdSe\cdot THF$	$C_{27}H_{25}O_2P$ Pd Se$\cdot\frac{1}{2}C_6H_6$
Formula weight	932.19	636.85
Temperature (K)	296(2)	293(2)
Radiation, wavelength (Å)	Mo–K_α, 0.71073	Mo–K_α, 0.71073
Crystal system, space group	Monoclinic, $P2_1/n$	Triclinic, $P\bar{1}$
Unit cell dimensions		
a (Å)	11.9351(6)	9.918(2)
b (Å)	24.9638(14)	10.358(2)
c (Å)	14.7617(8)	14.449(2)
α (°)	90	83.756(2)
β (°)	97.504(1)	71.953(2)
γ (°)	90	67.685(2)
Volume (Å^3)	4360.5(4)	1305.6(4)
Z, calculated density (Mg m^{-3})	4, 1.414	2, 1.620

Table 1 (*Continued*)

Reflections for cell parameters	21879	33
Absorption coefficient (mm^{-1})	1.374	2.192
Absorption correction method	Empirical (SADABS)	Empirical (ABSCAL)
T_{min}	0.64	0.48
T_{max}	0.80	0.65
$F(000)$	1888	638
Crystal size (mm)	$0.42 \times 0.28 \times 0.16$	$0.35 \times 0.28 \times 0.20$
Crystal colour	Colourless	Orange
Diffractometer type	Siemens SMART system	Philips PW1100
Scan type	Area detector	ω–2θ
θ range for data collection (°)	1.61–25.00	2.97–25.85
Index ranges		
	$-14 \le h \le 13$ $-23 \le k \le 29$ $-16 \le l \le 17$	$-11 \le h \le 11$ $-10 \le k \le 12$ $-17 \le l \le 1$
Reflections collected/unique	21879/7591 [$R_{int} = 0.0430$]	5713/4866 [$R_{int} = 0.0154$]
Refinement method	Full-matrix least-squares on F^2	Full-matrix least-squares on F^2
Data/restraints/parameters	7591/9/477	4866/0/304
Goodness-of-fit on F^2 (S)	1.062	1.106
Final R indices [$I > 2\sigma(I)$]	$R_1 = 0.0634$, $wR_2 = 0.1540$	$R_1 = 0.0376$, $wR_2 = 0.0968$
R indices (all data)	$R_1 = 0.0832$, $wR_2 = 0.1650$	$R_1 = 0.0533$, $wR_2 = 0.1121$
Weighting scheme	calc $w = 1/[\sigma^2(F_o^2) + (0.0818P)^2 + 11.7107P]$ where $P = (F_o^2 + 2F_c^2)/3$	calc $w = 1/[\sigma^2(F_o^2) + (0.0411P)^2 + 2.2539P]$ where $P = (F_o^2 + 2F_c^2)/3$
Maximum shift/esd	0.059	0.044
Largest difference peak and hole (e $Å^{-3}$)	1.675 and −1.043 close to Se	0.896 and −0.903 close to Pd

tals of **2a** amongst colourless crystals of **1a** that were manually separated under a microscope in a less than 5% yield.

trans-[Pd(OOC–CH_2–SMe–κ^2-*O*,*S*)Ph(PPh_3)] (**2a**). Dark yellow crystals in < 5% yield, m.p. 132°C (dec.). ^{1}H-NMR δ (d_1-chloroform, 298 K): 2.37 (s, 3H, SCH_3), 3.62 (s, 2H, CH_2S), 6.5–7.0 (m, 5H, Pd–C_6H_5), 6.8–7.3 (m, 15H, Pd–P(C_6H_5)$_3$). ^{13}C{^{1}H}-NMR δ (d_1-chloroform, 298 K): 20.4 (SCH_3), 40.5 (SCH_2), 123.1 (Pd–C_6H_5), 127.8 (Pd–C_6H_5), 128.4 (Pd–P(C_6H_5)$_3$), 129.4 (Pd–P(C_6H_5)$_3$), 130.6 (Pd–C_6H_5), 134.2 (Pd–P(C_6H_5)$_3$), 138.0 (Pd–P(C_6H_5)$_3$), 145.8 (Pd–C_6H_5). ^{31}P{^{1}H} δ (d_1-chloroform, 298 K): 27.3 (s). IR (KBr): ν_{as}(CO) 1631 cm^{-1} (s). FAB-MS: m/z 551 [M^+]. Anal. Calc. for $C_{27}H_{25}PPdO_2S$: C, 58.9; H, 4.6; S, 5.8. Found: C, 59.1; H, 4.7; S, 5.5%.

3.5. Preparation of *trans*-[Pd(OOC–{CH_2}$_2$–SR–κ^1-*O*)Ph(PPh_3)$_2$] (**1f** *R* = *Et*; **1g** *R* = *Ph*)

Complexes **1f** and **1g** were obtained in the same manner as complexes **1a**–**1e**, described in Section 3.3, with RS–(CH_2)$_2$–COOH (0.48 mmol, R = Et, Ph) as ligands. Careful layering of the concentrated solutions in THF with pentane, followed by cooling to −5°C,

Table 2
Selected bond lengths (Å)

1a		**2a**	
Pd–C(4)	1.998(3)	Pd–C(4)	2.007(3)
Pd–O(1)	2.112(2)	Pd–O(1)	2.1095(19)
Pd–P(1)	2.3367(7)	Pd–P	2.2827(8)
Pd–P(2)	2.3530(7)	Pd–S	2.3430(9)
O(1)–C(1)	1.264(4)	O(1)–C(1)	1.273(3)
O(2)–C(1)	1.217(4)	C(1)–O(2)	1.227(3)
C(1)–C(2a)	1.527(6)	C(1)–C(2)	1.524(4)
C(1)–C(2b)	1.674(15)	S–C(2)	1.813(3)
S(a)–C(2a)	1.792(7)	S–C(3)	1.799(4)
S(a)–C(3a)	1.672(15)		
S(b)–C(2b)	1.707(15)		
S(b)–C(3b)	1.63(3)		
1h		**2h**	
Pd–C(4)	2.011(6)	Pd–C(4)	2.007(4)
Pd–O(1)	2.104(4)	Pd–O(1)	2.101(3)
Pd–P(1)	2.3369(14)	Pd–P	2.2856(10)
Pd–P(2)	2.3336(14)	Pd–Se	2.4307(5)
O(1)–C(1)	1.262(8)	O(1)–C(1)	1.274(5)
O(2)–C(1)	1.222(8)	O(2)–C(1)	1.224(5)
C(1)–C(2)	1.503(13)	C(1)–C(2)	1.524(6)
Se(a)–C(2)	1.812(11)	Se–C(2)	1.944(5)
Se(a)–C(3)	1.881(11)	Se–C(3)	1.939(6)
Se(b)–C(2)	1.672(13)		
Se(b)–C(3)	1.878(13)		

Table 3
Selected bond angles (°)

1a		**2a**	
C(4)–Pd–O(1)	179.58(9)	C(4)–Pd–O(1)	170.92(8)
C(4)–Pd–P(1)	87.71(8)	C(4)–Pd–P	93.16(7)
O(1)–Pd–P(1)	91.87(5)	O(1)–Pd–P	95.56(6)
C(4)–Pd–P(2)	85.01(8)	C(4)–Pd–S	87.59(7)
O(1)–Pd–P(2)	95.40(5)	O(1)–Pd–S	83.93(6)
P(1)–Pd–P(2)	172.71(3)	P–Pd–S	175.29(2)
C(1)–O(1)–Pd	117.3(2)	C(1)–O(1)–Pd	121.71(17)
O(2)–C(1)–O(1)	126.2(3)	C(2)–S–C(3)	101.9(2)
O(2)–C(1)–C(2a)	115.4(4)	C(2)–S–Pd	97.85(10)
O(1)–C(1)–C(2a)	117.8(3)	C(3)–S–Pd	107.88(14)
O(2)–C(1)–C(2b)	126.4(5)	O(2)–C(1)–O(1)	124.7(3)
O(1)–C(1)–C(2b)	102.8(6)	O(2)–C(1)–C(2)	116.5(2)
C(1)–C(2a)–S(a)	109.7(4)	O(1)–C(1)–C(2)	118.7(2)
C(1)–C(2b)–S(b)	114.4(10)	C(1)–C(2)–S	115.3(2)
C(2a)–S(a)–C(3a)	100.4(5)		
C(2b)–S(b)–C(3b)	109.3(11)		
1h		**2h**	
C(4)–Pd–O(1)	177.0(2)	C(4)–Pd–O(1)	169.99(13)
C(4)–Pd–P(1)	88.79(16)	C(4)–Pd–P	93.59(11)
O(1)–Pd–P(1)	91.85(12)	O(1)–Pd–P	95.40(8)
C(4)–Pd–P(2)	87.22(16)	C(4)–Pd–Se	86.61(11)
O(1)–Pd–P(2)	92.42(12)	O(1)–Pd–Se	84.90(8)
P(1)–Pd–P(2)	173.34(5)	P–Pd–Se	174.19(3)
C(1)–O(1)–Pd	116.9(4)	C(1)–O(1)–Pd	124.1(3)
O(2)–C(1)–O(1)	126.4(7)	C(2)–Se–C(3)	99.0(3)
O(2)–C(1)–C(2)	121.8(8)	C(2)–Se–Pd	94.30(14)
O(1)–C(1)–C(2)	111.8(7)	C(3)–Se–Pd	103.9(2)
C(1)–C(2)–Se(a)	131.2(9)	O(2)–C(1)–O(1)	124.6(4)
C(1)–C(2)–Se(b)	119.9(8)	O(2)–C(1)–C(2)	116.2(4)
C(2)–Se(a)–C(3)	102.9(6)	O(1)–C(1)–C(2)	119.1(4)
C(2)–Se(b)–C(3)	108.8(6)	C(1)–C(2)–Se	115.3(3)

afforded light yellow and light violet crystals of complexes **1f** and **1g** respectively. Yields were moderate to low without attempting further crystallization from the mother liquid.

trans-[Pd(OOC–$(CH_2)_2$–SEt–κ^1-*O*)Ph(PPh_3)$_2$] (**1f**). Light yellow crystals in 45% yield, m.p. 175°C (dec.). ^{1}H-NMR δ (d_1-chloroform, 298 K): 1.2 (br, 3H, CH_3, S not coordinated), 1.1 (br 3H, CH_3, S coordinated), 2.4 (br, 2H, SCH_2CH_3, S not coordinated), 2.2 (br, 2H, SCH_2CH_3, S coordinated), 2.8 (br, 2H, CH_2S, S not coordinated), 1.2 (br, 2H, CH_2S, S coordinated), 3.2 (br, 2H, $OOCCH_2$, S not coordinated), 2.3 (br, 2H, $OOCCH_2$, S coordinated), 6.55 (d, 2H, ^3J 7.2 Hz, Pd–C_6H_5), 6.28 (t, 2H, ^3J 7.5 Hz, Pd–C_6H_5), 6.49 (t, 1H, ^3J 7.2 Hz, Pd–C_6H_5), 7.2–7.5 (m, 30H, Pd–$P(C_6H_5)_3$). ^{13}C{^{1}H}-NMR δ (d_1-chloroform, 298 K): 14.7 (br, CH_3), 25.2 (SCH_2CH_3), 25.5 (SCH_2CH_3), 27.4 (CH_2S), 27.8 (CH_2S), 37.5 (CH_2CH_2S), 40.0 (CH_2CH_2S), 121.8 (Pd–C_6H_5), 127.0 (Pd–C_6H_5), 127.9 (Pd–$P(C_6H_5)_3$), 129.7 (Pd–$P(C_6H_5)_3$), 130.3 (Pd–C_6H_5), 134.5 (Pd–$P(C_6H_5)_3$), 137.6 (Pd–$P(C_6H_5)_3$), 146.7 (Pd–C_6H_5), 175.7 (Pd–OCO). ^{31}P{^{1}H} δ (d_1-chloroform, 298 K): 21.7 (s, S not coordinated), 23.9 (s, S coordinated). IR (KBr): ν_{as}(CO) 1617 cm^{-1} (vs). Anal. Calc. for $C_{47}H_{44}P_2PdO_2S$: C, 67.1; H, 5.3; S, 3.9. Found: C, 66.9; H, 5.3; S, 3.9%.

trans-[Pd(OOC–$(CH_2)_2$–SPh–κ^1-*O*)Ph(PPh_3)$_2$] (**1g**). Light violet crystals in 32% yield, m.p. 139°C (dec.). ^{1}H-NMR δ (d_1-chloroform, 298 K): 1.4 (br, 2H, CH_2S, S not coordinated), 2.4 (br, 2H, CH_2S, S coordinated), 2.2 (br, 2H, $OOCCH_2$, S not coordinated), 3.2 (br, 2H, $OOCCH_2$, S coordinated), 6.57 (d, 2H, ^3J 7.2 Hz, Pd–C_6H_5), 6.30 (t, 2H, ^3J 7.2 Hz, Pd–C_6H_5), 6.51 (t, 1H, ^3J 7.2 Hz, Pd–C_6H_5), 7.0–7.8 (m, 35H, Pd–$P(C_6H_5)_3$ and SC_6H_5). ^{13}C{^{1}H}-NMR δ (d_1-chloroform, 298 K): 29.1 (CH_2S), 36.8 (CH_2CH_2S), 121.8 (Pd–C_6H_5), 125.0 (S–Ph), 127.0 (Pd–C_6H_5), 127.9 (Pd–$P(C_6H_5)_3$), 128.4 (S–Ph), 129.7 (Pd–$P(C_6H_5)_3$), 130.3 (Pd–C_6H_5), 130.8 (S–Ph), 134.4 (Pd–$P(C_6H_5)_3$), 135.9 (S–Ph), 137.3, 137.5 (Pd–$P(C_6H_5)_3$), 146.7 (Pd–C_6H_5), 175.1 (Pd–OCO). ^{31}P{^{1}H} δ (d_1-chloroform, 298 K): 21.8 (s, S not coordinated), 23.9 (s, S coordinated). IR (KBr): ν_{as}(CO) 1604 cm^{-1} (vs). FAB-MS: m/z 736 [$M^+ - 2Ph$]. Anal. Calc. for $C_{51}H_{44}P_2PdO_2S$: C, 68.9; H, 5.0; S, 3.6. Found: C, 68.7; H, 5.2; S, 3.7%.

3.6. Preparation of *trans*-[Pd(OOC–CH_2–SeR–κ^1-*O*)Ph(PPh_3)$_2$] (**1h** *R = Me;* **1i** *R = Ph*)

Complexes **1h** and **1i** were obtained in the same manner as complexes **1a**–**1e**, described in Section 3.3, with RSe–CH_2–COOH (0.48 mmol, R = Me, Ph) as ligands. Careful layering of the concentrated solutions in THF with pentane, followed by cooling to −5°C, afforded colourless crystals of complexes **1h** and **1i**. Yields were high without attempting further crystallization from the mother liquid.

trans-[Pd(OOC–CH_2–SeMe–κ^1-*O*)Ph(PPh_3)$_2$] (**1h**). Colourless crystals in 80% yield, m.p. 156.5–157.5°C. ^{1}H-NMR δ (d_1-chloroform, 298 K): 1.8 (br, 3H, $SeCH_3$), 2.8 (br, 2H, CH_2Se), 6.64 (d, 2H, ^3J 7.5 Hz, Pd–C_6H_5), 6.38 (t, 2H, ^3J 7.5 Hz, Pd–C_6H_5), 6.54 (t, 1H, ^3J 7.2 Hz, Pd–C_6H_5), 7.2–7.9 (m, 30H, Pd–$P(C_6H_5)_3$). ^{13}C{^{1}H}-NMR δ (d_1-chloroform, 298 K): 31.1 (CH_2Se), 122.2 (Pd–C_6H_5), 127.3 (Pd–C_6H_5), 128.2 (Pd–$P(C_6H_5)_3$), 129.8 (Pd–$P(C_6H_5)_3$), 131.4 (Pd–C_6H_5), 134.4 (Pd–$P(C_6H_5)_3$), 136.7 (Pd–$P(C_6H_5)_3$), 146.2 (Pd–C_6H_5), 175.8 (Pd–OCO). ^{31}P{^{1}H} δ (d_1-chloroform, 298 K): 16–27 (br). ^{77}Se{^{1}H} δ (d_1-chloroform, 223 K): 83.9. IR (KBr): ν_{as}(CO) 1600 cm^{-1} (vs). Anal. Calc. for $C_{45}H_{40}P_2PdO_2Se$: C, 62.8; H, 4.7. Found: C, 63.0; H, 4.8%.

trans-[Pd(OOC–CH_2–SePh–κ^1-*O*)Ph(PPh_3)$_2$] (**1i**). Colourless crystals in 75% yield, m.p. 154.5–155.5°C. ^{1}H-NMR δ (d_1-chloroform, 298 K): 2.7 (br, 2H, CH_2Se), 6.56 (d, 2H, ^3J 7.8 Hz, Pd–C_6H_5), 6.31 (t, 2H, ^3J 7.5 Hz, Pd–C_6H_5), 6.51 (t, 1H, ^3J 7.8 Hz, Pd–C_6H_5), 7.0–7.6 (m, 35H, Pd–$P(C_6H_5)_3$ and $Se(C_6H_5)$). ^{13}C{^{1}H}-NMR δ (d_1-chloroform, 298 K): 35.0 (CH_2Se),

125.4 (Pd–C_6H_5), 128.2 (Se–Ph), 128.4 (Se–Ph), 128.7 (Pd–$P(C_6H_5)_3$), 130.8 (Pd–$P(C_6H_5)_3$), 131.0 (Se–Ph), 132.1 (Pd–C_6H_5), 133.4 (Se–Ph), 134.4 (Pd–$P(C_6H_5)_3$), 135.9 (Pd–$P(C_6H_5)_3$), 174.1 (Pd–OCO). $^{31}P\{^1H\}$ δ (d_1-chloroform, 298 K): 18–28 (br). $^{77}Se\{^1H\}$ δ (d_1-chloroform, 223 K): 268.1. IR (KBr): ν_{as}(CO) 1611 cm^{-1} (vs). FAB-MS: m/z 922 [M^+]. Anal. Calc. for $C_{50}H_{42}P_2PdO_2Se$: C, 65.1; H, 4.6. Found: C, 65.0; H, 4.5%.

Table 4
Atomic coordinates ($\times 10^4$) and equivalent isotropic displacement parameters (Å $\times 10^3$) of complex **1a**, U_{eq} is defined as one third of the trace of the orthogonalized U_{ij} tensor

Atom	x	y	z	U_{eq}	Atom	x	y	z	U_{eq}
Pd	2809(1)	179	8050	34(1)	C(213)	5943(3)	1507(3)	9186(3)	78(1)
P(1)	1434(1)	431(1)	8230(1)	37(1)	C(214)	6679(3)	1327(3)	8972(3)	83(1)
P(2)	4129(1)	−250(1)	7819(1)	40(1)	C(215)	6648(3)	695(3)	8391(3)	88(2)
O(1)	3201(1)	1449(1)	8330(1)	48(1)	C(216)	5876(2)	238(2)	8013(3)	68(1)
O(2)	2543(2)	1813(1)	6954(2)	78(1)	C(221)	3953(2)	−323(2)	6655(2)	46(1)
S(a)	2777(2)	3602(2)	8068(2)	106(1)	C(222)	3360(2)	233(2)	6109(2)	47(1)
S(b)	2879(3)	3745(2)	7501(6)	105(3)	C(223)	3235(2)	243(2)	5229(2)	60(1)
C(111)	503(2)	504(2)	7220(2)	38(1)	C(224)	3687(3)	−307(3)	4884(2)	75(1)
C(112)	644(2)	759(2)	6466(2)	51(1)	C(225)	4272(3)	−866(3)	5409(3)	97(2)
C(113)	−64(2)	858(2)	5709(2)	66(1)	C(226)	4406(3)	−873(3)	6293(2)	81(1)
C(114)	−914(3)	696(3)	5692(2)	65(1)	C(231)	4587(2)	−1266(2)	8282(2)	42(1)
C(115)	−1067(2)	443(2)	6431(2)	65(1)	C(232)	4294(2)	−2027(2)	7871(2)	60(1)
C(116)	−364(2)	349(2)	7195(2)	54(1)	C(233)	4658(3)	−2779(2)	8247(3)	73(1)
C(121)	1047(2)	−346(2)	8859(2)	44(1)	C(234)	5298(2)	−2782(2)	9056(3)	67(1)
C(122)	1090(2)	−216(3)	9707(2)	59(1)	C(235)	5574(2)	−2042(2)	9486(2)	61(1)
C(123)	788(3)	−829(3)	10155(3)	80(1)	C(236)	5223(2)	−1292(2)	9103(2)	51(1)
C(124)	452(3)	−1565(3)	9764(3)	81(2)	C(1)	3004(2)	1963(2)	7698(3)	59(1)
C(125)	417(3)	−1718(3)	8932(3)	78(1)	C(2a)	3477(3)	2815(3)	7838(4)	58(1)
C(126)	711(2)	−1113(2)	8479(2)	63(1)	C(2b)	3136(10)	2903(8)	8192(10)	74(4)
C(131)	1408(2)	1430(2)	8775(2)	42(1)	C(3a)	1950(6)	3632(9)	7118(10)	217(11)
C(132)	752(2)	2036(2)	8456(2)	50(1)	C(3b)	1810(20)	3752(16)	6992(14)	106(9)
C(133)	774(3)	2783(2)	8901(3)	65(1)	C(4)	2430(2)	−1021(2)	7786(2)	42(1)
C(134)	1436(3)	2929(2)	9675(3)	70(1)	C(5)	2000(2)	−1272(2)	6937(2)	56(1)
C(135)	2089(3)	2340(3)	10001(2)	69(1)	C(6)	1732(3)	−2104(3)	6739(4)	83(1)
C(136)	2086(2)	1602(3)	9550(2)	58(1)	C(7)	1884(3)	−2690(3)	7387(4)	95(2)
C(211)	5121(2)	411(2)	8234(2)	47(1)	C(8)	2310(3)	−2458(3)	8229(4)	88(2)
C(212)	5163(2)	1046(2)	8821(2)	60(1)	C(9)	2582(2)	−1628(2)	8433(3)	61(1)

Table 5
Atomic coordinates ($\times 10^4$) and equivalent isotropic displacement parameters (Å $\times 10^3$) of complex **2a**, U_{eq} is defined as one third of the trace of the orthogonalized U_{ij} tensor

Atom	x	y	z	U_{eq}	Atom	x	y	z	U_{eq}
Pd	6616(1)	2739(1)	3520(1)	31(1)	C(133)	12162(3)	1373(3)	131(2)	51(1)
P	8070(1)	3428(1)	2153(1)	30(1)	C(134)	12218(4)	22(4)	163(3)	64(1)
O(1)	7098(2)	3781(2)	4494(1)	48(1)	C(135)	11090(5)	−330(4)	811(4)	97(2)
O(2)	6822(3)	4264(3)	6009(2)	74(1)	C(136)	9838(4)	687(3)	1430(3)	71(1)
S	5308(1)	1883(1)	4929(1)	42(2)	C(1)	6542(3)	3724(3)	5407(2)	45(1)
C(111)	7032(3)	4469(2)	1348(2)	33(1)	C(2)	5383(4)	2996(4)	5798(2)	55(1)
C(112)	7648(3)	4411(3)	344(2)	40(1)	C(3)	3312(4)	2559(6)	5023(3)	69(1)
C(113)	6857(4)	5357(3)	−213(2)	48(1)	C(4)	5881(3)	1730(3)	2773(2)	36(1)
C(114)	5461(4)	6354(3)	221(2)	53(1)	C(5)	4674(3)	2445(3)	2410(2)	43(1)
C(115)	4821(4)	6407(3)	1216(2)	49(1)	C(6)	3966(4)	1737(4)	2060(2)	53(1)
C(116)	5593(3)	5462(3)	1777(2)	40(1)	C(7)	4456(4)	296(4)	2050(2)	55(1)
C(121)	8950(3)	4592(3)	2423(2)	34(1)	C(8)	5651(4)	−438(3)	2404(2)	51(1)
C(122)	9835(3)	4136(3)	3047(2)	47(1)	C(9)	6351(3)	265(3)	2769(2)	42(1)
C(123)	10577(4)	4959(4)	3238(3)	61(1)	O(52)	9570(2)	10370(2)	5850(12)	263(9)
C(124)	10428(4)	6236(4)	2824(3)	64(1)	C(51)	8971(17)	9612(17)	5515(11)	126(4)
C(125)	9546(4)	6705(3)	2220(3)	59(1)	C(53)	10384(17)	10842(14)	5063(13)	125(4)
C(126)	8802(3)	5889(3)	2011(2)	43(1)	C(54)	10560(2)	10230(3)	4099(13)	214(10)
C(131)	9734(3)	2063(3)	1384(2)	35(1)	C(55)	9320(2)	9660(2)	4438(11)	171(7)
C(132)	10931(3)	2396(3)	735(2)	44(1)					

Table 6
Atomic coordinates ($\times 10^4$) and equivalent isotropic displacement parameters (Å $\times 10^3$) of complex **1h**, U_{eq} is defined as one third of the trace of the orthogonalized U_{ij} tensor

Atom	x	y	z	U_{eq}	Atom	x	y	z	U_{eq}
Pd	3836(1)	9019(1)	2526(1)	36(1)	C(215)	8109(7)	8443(4)	4591(6)	79(2)
P(1)	1998(1)	9206(1)	2818(1)	36(1)	C(216)	7500(5)	8445(3)	3711(5)	60(2)
P(2)	5714(1)	8802(1)	2414(1)	38(1)	C(221)	5978(5)	8180(3)	1820(4)	50(2)
O(1)	3983(3)	9774(2)	1919(3)	50(1)	C(222)	5910(6)	7693(3)	2243(6)	68(2)
O(2)	4546(6)	10135(2)	3275(3)	84(2)	C(223)	6044(8)	7216(3)	1779(8)	92(3)
Se(a)	4033(1)	11295(1)	2320(1)	90(1)	C(224)	6246(7)	7224(4)	897(9)	101(3)
Se(b)	5348(6)	11186(2)	2177(5)	183(3)	C(225)	6301(7)	7695(4)	459(6)	86(3)
C(111)	1900(5)	9294(2)	4032(4)	40(1)	C(226)	6161(5)	8180(3)	896(5)	64(2)
C(112)	871(6)	9219(3)	4380(4)	56(2)	C(231)	6468(5)	9308(2)	1840(4)	42(1)
C(113)	831(7)	9310(3)	5298(5)	78(2)	C(232)	7497(5)	9515(3)	2234(4)	50(2)
C(114)	1767(8)	9467(3)	5860(5)	81(2)	C(233)	8046(6)	9902(3)	1773(5)	59(2)
C(115)	2762(7)	9554(3)	5519(5)	71(2)	C(234)	7579(6)	10084(3)	928(5)	64(2)
C(116)	2833(5)	9465(3)	4606(4)	51(2)	C(235)	6572(6)	9882(3)	534(5)	66(2)
C(121)	1466(4)	9838(2)	2302(4)	42(1)	C(236)	6003(5)	9504(3)	982(4)	55(2)
C(122)	1089(5)	10251(2)	2821(5)	50(2)	C(1)	4336(6)	10154(3)	2442(5)	62(2)
C(123)	685(6)	10720(3)	2392(5)	65(2)	C(2)	4503(11)	10658(5)	1919(8)	128(4)
C(124)	649(6)	10780(3)	1470(6)	70(2)	C(3)	5116(10)	11445(5)	3332(8)	128(4)
C(125)	1036(6)	10380(3)	956(5)	70(2)	C(4)	3680(5)	8281(2)	3041(4)	44(1)
C(126)	1462(6)	9914(3)	1378(4)	58(2)	C(5)	3905(5)	8175(3)	3964(5)	55(2)
C(131)	877(4)	8721(2)	2454(4)	41(1)	C(6)	3777(7)	7660(3)	4300(6)	78(2)
C(132)	34(5)	8810(3)	1736(5)	57(2)	C(7)	3416(7)	7254(3)	3724(8)	85(3)
C(133)	−786(6)	8426(3)	1473(6)	72(2)	C(8)	3193(7)	7347(3)	2813(7)	82(3)
C(134)	−755(6)	7952(3)	1925(6)	71(2)	C(9)	3317(6)	7861(3)	2470(5)	62(2)
C(135)	56(6)	7854(3)	2637(6)	69(2)	O(51)	8035(15)	1401(7)	9908(13)	259(7)
C(136)	874(5)	8233(3)	2907(5)	54(2)	C(51)	6856(14)	1446(8)	9964(13)	203(7)
C(211)	6532(5)	8750(2)	3542(4)	43(1)	C(52)	6910(2)	1989(10)	10440(2)	338(15)
C(212)	6198(5)	9058(3)	4240(4)	54(2)	C(53)	8010(2)	2105(11)	10139(19)	298(13)
C(213)	6817(7)	9050(3)	5100(5)	72(2)	C(54)	8140(4)	1625(12)	10790(15)	500(3)
C(214)	7744(8)	8730(4)	5277(5)	80(2)					

Table 7
Atomic coordinates ($\times 10^4$) and equivalent isotropic displacement parameters (Å $\times 10^3$) of complex **2h**, U_{eq} is defined as one third of the trace of the orthogonalized U_{ij} tensor

Atom	x	y	z	U_{eq}	Atom	x	y	z	U_{eq}
Pd	3326(1)	2288(1)	1455(1)	36(1)	C(132)	−948(5)	2600(5)	4215(4)	53(1)
P	1918(1)	1565(1)	2834(1)	35(1)	C(133)	−2183(5)	3612(6)	4820(4)	57(1)
O(1)	2935(4)	1192(3)	486(2)	50(1)	C(134)	−2214(7)	4923(7)	4814(5)	84(2)
O(2)	3141(4)	672(4)	−1009(2)	64(1)	C(135)	−1089(10)	5257(7)	4195(7)	146(5)
Se	4590(1)	3262(1)	−7(1)	44(1)	C(136)	154(8)	4262(6)	3578(6)	108(3)
C(111)	1050(5)	418(4)	2577(3)	38(1)	C(1)	3435(5)	1240(5)	−437(3)	46(1)
C(112)	1134(5)	−843(5)	3042(3)	47(1)	C(2)	4520(7)	2010(6)	−886(3)	57(1)
C(113)	400(6)	−1633(5)	2853(4)	60(1)	C(3)	6730(6)	2407(7)	−75(4)	68(1)
C(114)	−455(6)	−1166(6)	2215(4)	66(2)	C(4)	4036(5)	3306(4)	2196(3)	40(1)
C(115)	−565(6)	74(7)	1749(5)	65(1)	C(5)	3510(6)	4761(5)	2216(3)	48(1)
C(116)	192(5)	868(5)	1923(3)	51(1)	C(6)	4183(6)	5454(5)	2590(3)	54(1)
C(121)	2984(5)	510(4)	3656(3)	37(1)	C(7)	5420(6)	4723(6)	2920(3)	58(1)
C(122)	4438(5)	−449(5)	3236(3)	45(1)	C(8)	5963(6)	3294(6)	2891(3)	58(1)
C(123)	5214(6)	−1392(5)	3801(4)	55(1)	C(9)	5279(5)	2588(5)	2535(3)	48(1)
C(124)	4585(6)	−1372(6)	4801(4)	59(1)	C(51)	936(11)	5552(10)	9327(7)	119(3)
C(125)	3171(6)	−393(5)	5224(3)	52(1)	C(52)	246(12)	6059(13)	10239(8)	139(4)
C(126)	2372(5)	542(5)	4656(3)	44(1)	C(56)	636(13)	4535(12)	9059(9)	134(3)
C(131)	257(5)	2906(5)	3602(3)	41(1)					

3.7. Preparation of trans-[Pd(OOC–CH_2–SeMe–κ^2-O,Se)Ph(PPh_3)] (**2h**)

Prolonged crystallization of **1h** from benzene–pentane at 5°C afforded small amounts of dark yellow crystals of **2h** amongst colourless crystals of **1h** that were manually separated under a microscope in a less than 5% yield.

trans - [Pd(OOC – CH_2 – SeMe – κ^2 - *O*,*Se*)Ph(PPh_3)] (**2h**). Dark yellow crystals in $< 5\%$ yield, m.p. 165.5–166.5°C. IR (KBr): ν_{as}(CO) 1621 cm^{-1} (s). Anal. Calc. for $C_{27}H_{25}PPdO_2Se$: C, 54.2; H, 4.2. Found: C, 54.0; H, 3.8%.

4. Supplementary material

Crystallographic data for the structures reported in this paper have been deposited with the Cambridge Crystallographic Data Centre, CCDC nos. 132643–132646. Copies of this information may be obtained free of charge from the Director, CCDC, 12 Union Road, Cambridge, CB2 1EZ, UK (fax: +44-1223-336-033; e-mail: deposit@ccdc.cam.ac.uk or http://www.ccdc.cam.ac.uk).

Acknowledgements

We thank the FRD for financial support. The measurement of NMR spectra by Dr L. van der Merwe and Mr I. Vorster is gratefully acknowledged.

References

[1] A. Bader, E. Lindner, Coord. Chem. Rev. 108 (1991) 27.
[2] J.C. Jeffrey, T.B. Rauchfuss, Inorg. Chem. 18 (1979) 2658.
[3] S. Mecking, W. Keim, Organometallics 15 (1996) 2650.
[4] J.A. Davies, F.R. Hartley, Chem. Rev. 81 (1981) 79.
[5] E. Lindner, B. Karle, Chem. Ber. 123 (1990) 1469.
[6] R.E. Rülke, V.E. Kaasjagter, P. Wehman, C.J. Elsevier, P.W.N.M. van Leeuwen, K. Vrieze, J. Fraanje, K. Goubitz, A.L. Spek, Organometallics 15 (1996) 3022.
[7] A. Pfaltz, P. von Mall, Angew. Chem. 105 (1993) 614.
[8] C. Abu-Gnim, I. Amer, J. Mol. Catal. 85 (1993) L275.
[9] G.P.C.M. Dekker, A. Buijs, C.J. Elsevier, K. Vrieze, P.W.N.M. van Leeuwen, W.J.J. Smeets, A.L. Spek, Y.F. Wang, C.H. Stam, Organometallics 11 (1992) 1937.
[10] M. Bressan, C. Bonuzzi, F. Morandini, A. Morvillo, Inorg. Chim. Acta 182 (1991) 153.
[11] J.R. Dilworth, A.J. Hutson, J.S. Lewis, J.R. Miller, Y. Zheng, Q. Chen, J. Zubieta, J. Chem. Soc. Dalton Trans. (1996) 1093.
[12] S.Y. Desjardins, K.J. Cavell, H. Jin, B.W. Skelton, A.H. White, J. Organomet. Chem. 515 (1996) 233.
[13] G.J.P. Britovsek, K.J. Cavell, W. Keim, J. Mol. Catal. A: Chem. 110 (1996) 77.
[14] J.L. Hoare, K.J. Cavell, R. Hecker, B.W. Skelton, A.H. White, J. Chem. Soc. Dalton Trans. (1996) 2197.
[15] W.H. Meyer, R. Brüll, H.G. Raubenheimer, C. Thompson, G.J. Kruger, J. Organomet. Chem. 553 (1998) 83.
[16] L. Malatesta, M. Angoletta, J. Chem. Soc. (1957) 1186.
[17] J. Chatt, F.A. Hart, H.R. Watson, J. Chem Soc. (1962) 2537.
[18] D.A. White, G.W. Parshall, Inorg. Chem. 9 (1970) 2358.
[19] S. Okeya, T. Miyamoto, S. Ooi, Y. Nakamura, S. Kawaguchi, Bull. Chem. Soc. Jpn. 57 (1984) 395.
[20] W.A. Herrmann, C. Broβner, T. Priermeier, K. Öfele, J. Organomet. Chem. 481 (1994) 97.
[21] L. Ramberg, Ber. 40 (1907) 2588.
[22] P. Mooradian, J. Am. Chem. Soc. 17 (1949) 3372.
[23] J. Stratling, H.J. Backer, Recl. Trav. Chim. Pays-Bas 73 (1954) 709.
[24] L. Ramberg, Z. Phys. Chem. 34 (1909) 562.
[25] R.J. Irving, W.C. Fernelius, J. Phys. Chem. 60 (1956) 1427.
[26] F. Krollpfeifer, H. Schultze, Ber. 56B (1923) 1821.
[27] M.J. Dubdoub, P.G. Guerrero, Jr, C.C. Silveira, J. Organomet. Chem. 460 (1993) 31.
[28] L.A. Silks III, J.D. Odom, R.B. Dunlap, Synth. Commun. 21 (1991) 1105.
[29] G.M. Sheldrick, SADABS, Program for Empirical Absorption Correction of Area-Detector Data, University of Göttingen, Germany, 1996.
[30] M. Gomm, PWPC v 1.12/H, Control Program for PW1100 Diffractometer, Institut für Angewandte Physik, Erlangen, Germany, 1998.
[31] S.R. Hall, G.S.D. King, J.M. Stewart (Eds.), Xtal 3.4 Reference Manual, University of Western Australia, Lamb, Perth, 1995.
[32] A.J.C. Wilson (Ed.), International Tables for Crystallography, vol. C, Mathematical, Physical and Chemical Tables, Kluwer, Dordrecht, 1992.
[33] G.M. Sheldrick, SHELX-97, Program for Crystal Structure Determination and Refinement, Institüt für Anorganische Chemie der Universität Göttingen, Göttingen, Germany, 1997.
[34] L.J. Farrugia, ORTEP-3 for Windows, J. Appl. Crystallogr. (1997) 565.